User Tracking for Access Control with Bluetooth Low Energy

Robert Heyn[1], Marc Kuhn[1], Henry Schulten[1], Gregor Dumphart[1],
Janick Zwyssig[1], Florian Trösch[2], and Armin Wittneben[1]
[1]Communication Technology Lab, ETH Zurich, Switzerland
[2]The PORT Technology, Schindler Aufzüge AG, Switzerland
{heyn, kuhn, schulten, dumphart, wittneben}@nari.ee.ethz.ch, florian.troesch@schindler.com

***Abstract*—The Received Signal Strength Indicator (RSSI) of Bluetooth Low Energy (BLE) is a popular means for indoor user localization and tracking as it reflects the transmitter-receiver distance and is readily available in all current smartphones. Since fading, shadowing and antenna patterns cause severe RSSI fluctuations, many RSSI-based localization systems use fingerprinting instead of parameter estimation based on a channel model (e.g. trilateration from distance estimates). Fingerprinting however requires a large effort for training data acquisition and frequent updates in dynamic environments. In this paper we focus on wireless access control with BLE. We demonstrate that a practical implementation of such a tracking system can meet the typical demands of generic access control problems with low-complexity parameter estimation techniques, namely trilateration and optional Kalman filtering. Thereby, satisfactory accuracy is enabled by diversity (averaging in space, time and frequency), calibration and appropriate observation space modeling. We find that including the RSSI directly in the observation space renders trilateration obsolete, which reduces complexity even further.**

***Index Terms*—access control, Bluetooth Low Energy, Extended Kalman Filter, IoT, localization, RSSI, tracking**

I. Introduction

Automatic access control is becoming increasingly relevant in logistics and corporate sectors. Wireless access control systems have low infrastructure demands, can be implemented at low cost, are easy to use and have synergies with other services such as indoor navigation. Bluetooth Low Energy (BLE) as a promising solution for such systems has been studied intensively for localization and user tracking. Its low power demand, low complexity using automatic monitoring of the Received Signal Strength Indicator (RSSI), and its widespread availability in consumer devices make it attractive. However, due to fluctuations in RSSI observations, the accuracy of distance estimates and subsequent position estimates is limited. [1].

A common approach to combat this issue for RSSI-based position estimation is fingerprinting, i.e. comparing measured RSSI with previously recorded training data to obtain a position estimate [2]. This principle has been extended, with methods like deep learning [3] or K-means clustering [4]. However, fingerprinting requires an extensive training phase to allow for reliable position estimation [5] and is sensitive to changes in the environment [6].

Another common localization method is trilateration, which has also been demonstrated for BLE: In an ideal environment, i.e. without shadowing by users or objects, interference, or multipath propagation, static BLE devices were located with an accuracy of up to $0.2\,\mathrm{m}$ using smoothed and filtered RSSI values [1] for distance estimation. The setup however did not resemble scenarios for large-scale user tracking. Dynamic user tracking under realistic conditions is more challenging and therefore often supported by additional sensor data from the BLE device. Bae et al. [7] used BLE and dead reckoning with information from an inertial measurement unit (IMU) to track a slowly moving mobile robot with a constrained Extended Kalman Filter (EKF). However, tracking a less regular and less predictable human walk imposes a greater challenge. Classic Bluetooth with a higher transmit power and strong support of 3D compass data enabled accurate tracking of a human user ($\mathrm{RMSE} \approx 0.7\,\mathrm{m}$) [8] at the cost of limitations of Classic Bluetooth, such as higher energy demand and a limited number of devices. RSSI and IMU data were fused in a computationally expensive Particle Filter.

To address the described shortcomings of the existing approaches, we propose and demonstrate a BLE RSSI-based access control system to show that BLE allows reliable solutions for access control problems. We provide recommendations for anchor deployment, diversity measures and calibration. Furthermore, we introduce two EKF-based tracking approaches: One uses position estimates obtained via trilateration while the other is directly RSSI-based without explicit position estimation. This direct method has significantly lower computational complexity as it avoids the optimization problem associated with trilateration.

The remaining paper is structured as follows: Section II introduces the access control problem and the relevant signal processing steps. A discussion of the experimental results for different movement patterns is provided in Section III. Some aspects regarding the filters are covered in detail in Section IV. Section V concludes our work.

II. System Architecture

We studied the access control problem by means of a representative setup, in a room whose floor plan is shown

This work was partially supported by the Commission for Technology and Innovation CTI, Switzerland, and conducted in cooperation with Schindler Aufzüge AG.

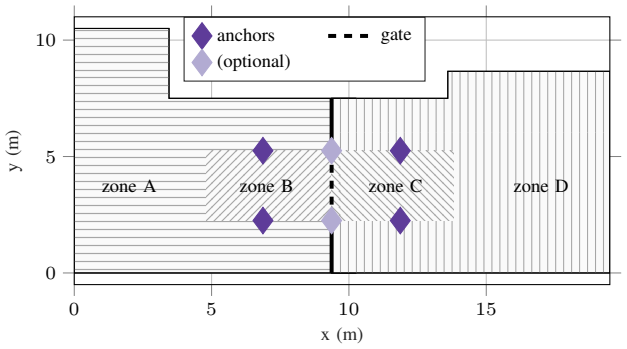

Fig. 1: Floor plan of the indoor gate scenario

in Fig. 1. It was divided into four zones: The zones B and C between static receivers at known coordinates ("anchors") formed the gate area, i.e. authorized users typically walk from zone A through the gate via B and C into D. When a user ("agent") enters zone B, the system typically needs to observe the user's position in order to make a decision (e.g. unlock/open a door separating zones B and C). Assuming that certain users are only allowed to access a subset of these zones, the goal of our user tracking system was to decide which zone a user was in and where he/she was heading to. Authentication, identification and authorization of users could be implemented over the same BLE link.

In the following, we describe the key aspects of our studied system. Considerations on diversity and anchor density are based on the findings in [9]. Raspberry Pis mounted on tripods at the same height ($h \approx 1.2\,\mathrm{m}$) served as BLE observers (anchors), while an iPhone served as a mobile BLE advertiser (agent). The anchors were connected to a central entity which evaluated the measurements. All devices used the BLE 4.2 standard.

A. Channel Model

An accurate channel model is essential to compute distance estimates from RSSI measurements. Following the exposition of [9], the RSSI in indoor environments is adequately represented by a log-normal model

$$\mathrm{RSSI}_i(d) = \mathrm{RSSI}_{d_0} - 10\,\alpha_i\,\log_{10}\left(\frac{d_i}{d_0}\right) + W \qquad (1)$$

for our application featuring temporal, spectral and spacial diversity as listed in Section II-B. The measured RSSI (in dBm) at a distance d_i from the anchor i depends on the path loss coefficient α_i and the RSSI (in dBm) at a reference distance d_0, denoted by RSSI_{d_0}. Multipath propagation, shadowing and radiation patterns of the antennas cause fluctuations of the RSSI. Taking these phenomena into account, the i.i.d. random variable W can be assumed as Gaussian distributed if sufficient diversity measures are employed. A detailed look at the statistics of BLE indoor channels is provided in [9].

B. Diversity

Indoor propagation in the $2.4\,\mathrm{GHz}$ band exhibits frequency-selective fading. For advertising and RSSI acquisition, BLE uses three narrowband channels with large frequency separation. Thus, RSSI values may vary strongly between the channels even for static measurements so that reliable unambiguous distance estimation is impossible [9]. Consequently, we averaged the RSSI values gathered from all three channels over multiple received advertising packets to exploit both frequency and time diversity. Furthermore, deploying multiple antennas per device allows to exploit spatial diversity given a sufficient distance between the antennas (at least half a wavelength). These means of diversity reduce RSSI fluctuations and thus improve the accuracy of distance estimates.

C. Calibration

Various calibration procedures have been proposed, e.g. in [9], but we choose a simple and straightforward method here: Path loss coefficient α can be estimated from (1) after recording a sufficiently large data set at various positions. In particular, we recorded such calibration datasets in a calibration phase while walking along known trajectories to cover different shadowing situations and various angles of the antenna patterns. Using least squares regression, we estimate path loss coefficient α_i and reference $\mathrm{RSSI}_{d_0,i}$ from the measured RSSI values and the corresponding distances separately for each anchor i. These estimated parameters were saved and later used for distance estimation in the measurement phase. For the proposed access control gate, an intuitive calibration trajectory is a straight walk through the gate, as it covers the area of interest. It can be expected that measurements in online operation will resemble the calibration measurements well. The system performance evaluation in Section III is based on a straight calibration walk through the centre of the gate.

D. Position Estimation and Anchor Selection

The maximum likelihood (ML) position estimate from RSSI measurements that are according to the log-normal model (1) is computed as [9]

$$\hat{\mathbf{p}}_{\mathrm{ML}} = \arg\min_{\mathbf{p}} \sum_{i=1}^{N_\mathrm{A}} w_i \left(\log d_i(\mathbf{p}) - \log \hat{d}_i\right)^2. \qquad (2)$$

where N_A denotes the number of anchors. The distance between anchor i and a position $\mathbf{p}$ is denoted $d_i(\mathbf{p})$, and $\hat{d}_i = d_0\,10^{(\mathrm{RSSI}_i - \mathrm{RSSI}_{d_0}/10\alpha)}$ is the corresponding distance estimate computed from the measurements. The weighting factors for each anchor $w_i = \frac{\alpha_i^2}{\sigma_i^2}$ for the ML estimate depend on the variance of received RSSI σ_i^2 and are obtained from calibration. Distance estimates based on the model (1) are more reliable in proximity to an anchor as the RMSE (and the associated Cramér-Rao lower bound) increases linearly with the distance [9], [10]. A locally high anchor density yields a sufficient number of reliable measurements and thus allows to neglect unreliable estimates from distant anchors. Selecting the three anchors with the highest RSSI ($w_i = 1$) for trilateration and discarding the other measurements ($w_i = 0$) instead of computing the ML estimate has shown to be a more robust approach in our experiments, which was thus used throughout the evaluation.

E. Temporal Filtering

Simple temporal filters can compensate for outliers in position estimates. Smoothing the position estimates, e.g. by averaging over multiple measurements, can be seen as a simple example for a temporal filter. In our most basic tracking approach, we smoothed localization results with a moving median coordinate-wise over five position estimates.

More advanced temporal filtering methods include (but are not limited to) Kalman Filters for user tracking, which have been widely used in the literature [11]. For linear models, a simple Kalman Filter is suitable, whereas non-linear models like in this work require the use of more advanced filters. Hence we used the Extended Kalman Filter (EKF), which achieved a satisfactory accuracy at a reasonably low computational effort compared to, e.g., a Particle Filter.

Kalman filters operate with alternating prediction and measurement steps, which require a state space $\mathbf{x}$ and state update function $\mathbf{f}$, and an observation space $\mathbf{z}$ and a measurement function $\mathbf{h}$, respectively [11]. Throughout this paper, we consider the state vector $\mathbf{x}_k$ at time index k as

$$\mathbf{x}_k = \left[\mathbf{p}_k^{\mathrm{T}},\, \|\mathbf{v}_k\|,\, \phi_k\right]^{\mathrm{T}} \in \mathbb{R}^4 \tag{3}$$

and the state transition function $\mathbf{f}_k(\mathbf{x}_k^-)$ as

$$\mathbf{f}_k(\mathbf{x}_k^-) = \begin{bmatrix} \mathbf{p}_k^- + \mathbf{v}_k^-\,\Delta t \\ \left\|\mathbf{v}_k^-\right\| \\ \phi_k^- \end{bmatrix} \in \mathbb{R}^4, \tag{4}$$

where $\mathbf{p}_k$ denotes the 2D position vector of the agent, $\|\mathbf{v}_k\|$ the magnitude of its velocity, and ϕ_k its orientation angle relative to the x-axis of the selected coordinate system. Identifying the direction of a user's movement allows to predict his/her intention, which is useful for various access control applications. As an example, consider controlling an automatic door, which opens/unlocks only when an authorized user intends to pass.

Regarding the choice of measurement vector and observation function, we considered two different approaches (which give rise to two different user tracking algorithms): (i) a position-based approach using trilateration with the best three anchors as described in Section II-D, subsequently denoted with index "tri", and (ii) a directly RSSI-based approach without explicit position estimation, similar to the method used in [12] and subsequently denoted with index "dir". The respective measurement vectors are given by

$$\mathbf{z}_{k,\mathrm{tri}} = \hat{\mathbf{p}}_k \tag{5}$$

$$\mathbf{z}_{k,\mathrm{dir}} = \left[\mathrm{RSSI}_{1,k},\, \ldots,\, \mathrm{RSSI}_{N_\mathrm{A},k}\right]^{\mathrm{T}} \tag{6}$$

whereby $\hat{\mathbf{p}}_k$ is a position estimate obtained from trilateration. The respective observation functions are

$$\mathbf{h}_{k,\mathrm{tri}}(\hat{\mathbf{x}}_k^-) = \mathbf{p}_k^- \tag{7}$$

$$\mathbf{h}_{k,\mathrm{dir}}(\hat{\mathbf{x}}_k^-) = \begin{bmatrix} \mathrm{RSSI}_{\mathrm{ref},1} - 10\alpha_1 \log_{10}\left(\frac{d_1(\mathbf{p}_k^-)}{d_{\mathrm{ref},1}}\right) \\ \vdots \\ \mathrm{RSSI}_{\mathrm{ref},N_\mathrm{A}} - 10\alpha_{N_\mathrm{A}} \log_{10}\left(\frac{d_{N_\mathrm{A}}(\mathbf{p}_k^-)}{d_{\mathrm{ref},N_\mathrm{A}}}\right) \end{bmatrix} \tag{8}$$

with the previous position $\mathbf{p}_k^-$. It shall be noted that an EKF is optimal for Gaussian-distributed measurements. While this is not necessarily the case for trilateration results, the directly RSSI-based approach meets this assumption according to model (1).

III. Performance Evaluation

In order to evaluate the performance of the proposed methods, the gate constellation was set up in a large room (approx. $19\,\mathrm{m} \times 9\,\mathrm{m}$) as shown in Fig. 2.

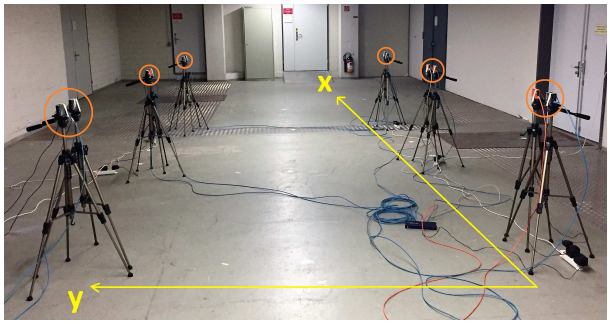

Fig. 2: Photo of the gate with six anchors (orange markers) as used in the later scenarios. For four-anchor operation, unused devices were switched off.

In our experiments, the raw RSSI values were transferred to a computer and evaluated in Matlab. As only one RSSI value was recorded per received BLE packet, we needed to receive and process several packets to obtain a distance estimate with sufficient diversity.

As selected trajectories for evaluation, we focussed on typical movement patterns in a realistic access control scenario, i.e. a user crossing the gate or turning around at some point within the gate. Since the gate could be accessed from both sides, the starting point of the trajectory could be in zone A or D. We analysed the exemplary case of a user starting in zone A. For all measurements, the agent device was held in hand in front of the human body at the height of the anchors, with the screen pointing upwards. We aimed to identify in which zone the user is.

The particular scenario of application determines the tolerance towards zone localization errors per coordinate. For instance, the detection of unauthorized intruders in zone C/D requires higher accuracy in x-direction. In case of an automatic door between zones B and C, the accuracy in y-direction is important to decide correctly whether to open the door (user in zone B/C) or keep it closed (user in zone A/D).

First, we evaluated the performance of a simple approach with smoothed position estimates. Afterwards, we successively extended the system to more advanced implementations.

A. Using simple moving median for temporal filtering

1) Straight Crossing Trajectory: First, we investigated a simple setup of four anchors with one antenna each, i.e. without spatial diversity. Starting with a very generic movement

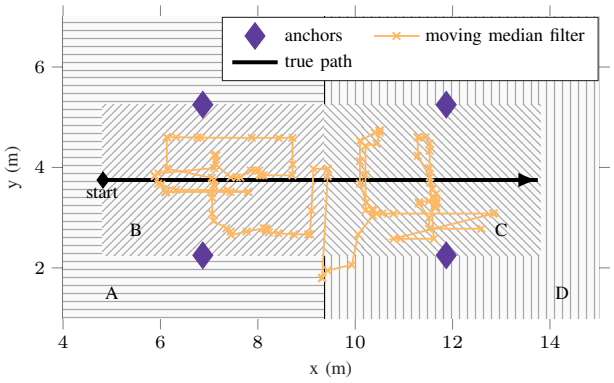

(a) Trajectory

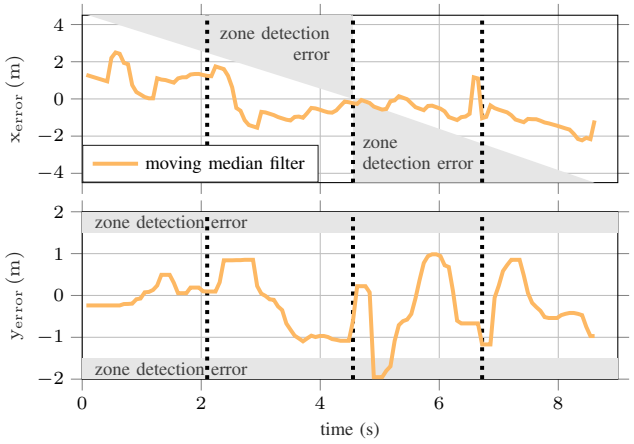

(b) Tracking error. Black dotted lines mark the times of the user passing the anchors (left, right) and the time of leaving zone B / entering zone C (center).

Fig. 3: Moving-median-tracking results for a straight walk

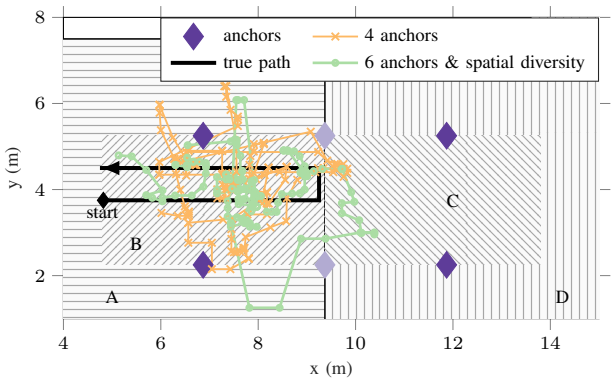

(a) Trajectories for 4 and 6 anchors

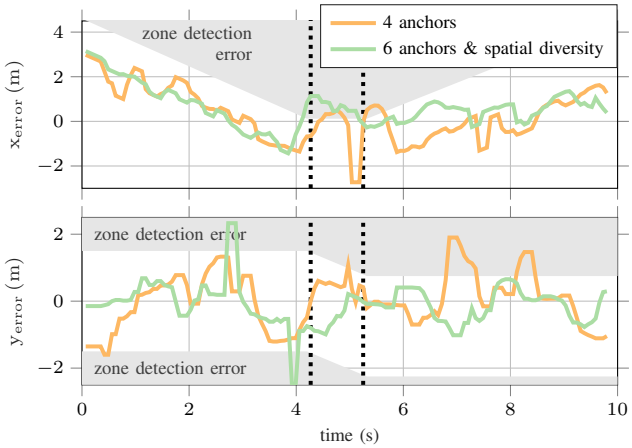

(b) Tracking error. Black dotted lines mark the turns.

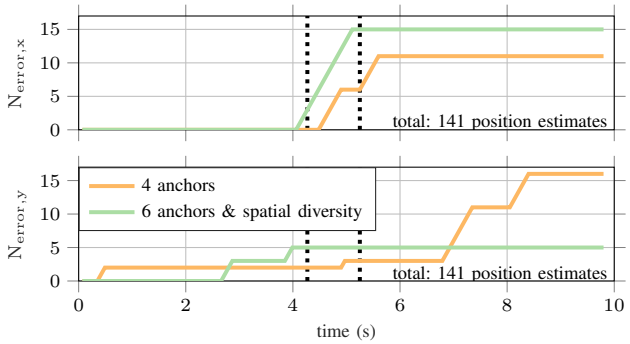

(c) Cumulated number of errors.
Black dotted lines mark the turns.

Fig. 4: Moving-median-tracking results for a turn

trajectory, we evaluated the system performance for a user walking straight through zones B and C.

As we see from Fig. 3a, position estimates exhibited a significant spread and showed large deviations from the true path. However, most position estimates still lay within the gate area of zones B and C. Clearly, the distance to a zone edge (here especially the threshold between B and C) determines the tolerable position estimation error: The closer the agent comes to a zone edge in x- or y-direction, the smaller the position error in the respective coordinate may be in order to still detect the zone correctly. Fig. 3b shows the position estimation errors over time. The error tolerance in the respective coordinate is taken into account by the areas marked in gray: Before crossing the threshold between zones B and C at $t \approx 4.5\,\mathrm{s}$, a zone detection error occurs if the x-coordinate of the estimated position is too large. Afterwards, it may not be estimated too low to avoid a zone detection error. Similarly, the y-coordinate must neither be estimated too large nor too small. From Fig. 3b, we can see that in spite of errors beyond $2\,\mathrm{m}$, most position estimates were located in the correct zone. With a total number of four zone detection errors in x-direction and five in y-direction occurring in the centre of the gate, the simple system performed well for this trajectory. With a trajectory matching the calibration walk and a considerable distance to most zone borders, the scenario described previously is not particularly demanding in terms of zone detection.

2) Turn Trajectory: A more challenging situation evolves if the user turns around within the area of interest, right (in our case: $12\,\mathrm{cm}$) before the border of zones B and C, as shown in Fig. 4a. The most critical part of this movement pattern is

the section along the zone border between B and C, as the error tolerance in x-direction is very low for this part of the trajectory. When the user is walking back towards zone A, the proximity to the upper border between A and B reduces the tolerance in y-direction. Furthermore, the calibration trajectory and the path under observation did not match anymore after the first turn.

Looking at the error distribution over time (Fig. 4b and 4c), we observe that after the first turn, the user was falsely detected in zone C (error in x-direction), while during the return towards A, errors in y-direction occurred, mostly due to the proximity to the zone edge of A/B.

In order to improve the poor position estimation, we then used spatial diversity in addition to frequency and time diversity by equipping all anchors with two antennas spaced about $2\lambda = 24\,\mathrm{cm}$ apart, as shown in Fig. 2. Furthermore, we deployed two additional anchors at the zone border between B and C (depicted in light purple in Fig. 4a). As a consequence of the additional anchors and spatial diversity, the number of zone detection errors in y-direction was reduced significantly with this advanced setup.

Note that distance estimates in radial direction from the anchor are most accurate [9]. However, in order not to obstruct the gate, anchors must not be placed at either end of the aisle, which would yield accuracy improvement in x-direction. Placing the anchors on the ceiling could help to mitigate this problem, but extends the scenario to 3D and may be subject to architectural limitations such as too high ceilings.

B. Using EKF without IMU

Various wireless access control situations require tracking the user's movement over time, which was not feasible from the previous results and thus demanded further extension of the six-anchor-system with smoothed position estimation. As pointed out in Section II-E, the EKF does not smooth RSSI measurements but tracks the agent's state over time. This allows a prediction of the user's movement direction and in consequence assumptions of his/her intention. In the following, we look at the previously discussed movement patterns again to evaluate the performance of the two EKF approaches.

1) Straight Crossing Trajectory: Looking at the straight walk through the gate again, we observe from Fig. 5a that both filters were able to correct an initialization offset (for details see Section IV-B) and tracked the user accurately with small errors in both coordinate directions (see Fig. 5b). Thus, it was possible here to predict the user's intention, which enables orientation-dependent decisions such as automatic door opening.

As the markers in Fig. 5a show, the trilateration-based method followed the true path in zone C with a certain delay, which induced four zone detection errors. The directly RSSI-based approach showed no such lag and consequently yielded only two errors after the transition from zone B to C. However, both filters performed well in this experiment. The motion model of the filters matched the agent's movement and compensated for outliers in position estimation and RSSI,

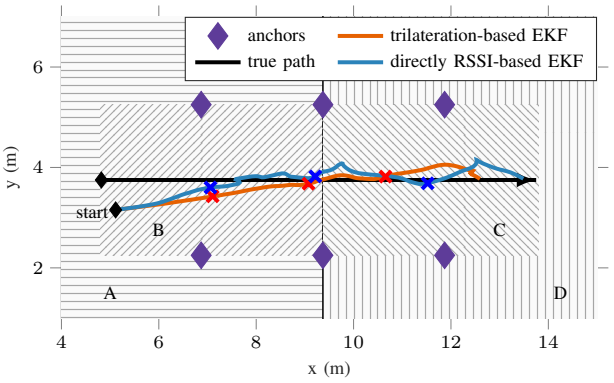

(a) Trajectories with marked position estimates at the time of the agent passing the anchors.

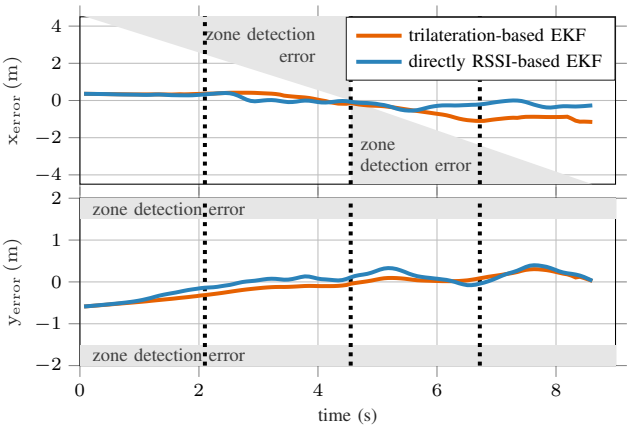

(b) Tracking error. Black dotted lines mark the time of the agent passing the anchors.

Fig. 5: EKF tracking results for a straight walk

which otherwise would have deteriorated the performance of the trilateration-based and the direct approach, respectively.

2) Turn Trajectory: Similar results could be observed for the more challenging situation of the turn. As we can see from Fig. 6a, both filter variants corrected the initialization offset to a certain extend and roughly followed the true trajectory. The inherent inertia of the filters is also clearly visible, as both trajectories cross the border between zones B and C. The linear movement model of the EKF failed to quickly adapt to sudden changes of the movement patterns, such as stops or turns. As the agent was assumed to move on in a straight way, several measurements were required to correct the faulty predictions of the model. This inertia caused zone detection errors, as Fig. 6b and 6c show: Errors occurred from the time of the first turn until the orientation in the state vector was corrected and the position estimates were in zone B again, i.e. after about $2\,\mathrm{s}$ (direct) to $3\,\mathrm{s}$ (trilateration). Errors in y-direction did not occur, as outliers of the position estimates were compensated for by the movement model prediction.

With the lower computational effort, the higher tracking accuracy (cf. Fig. 6a), the lower inertia and thus fewer zone detection errors (24 vs. 43), the direct approach outperformed

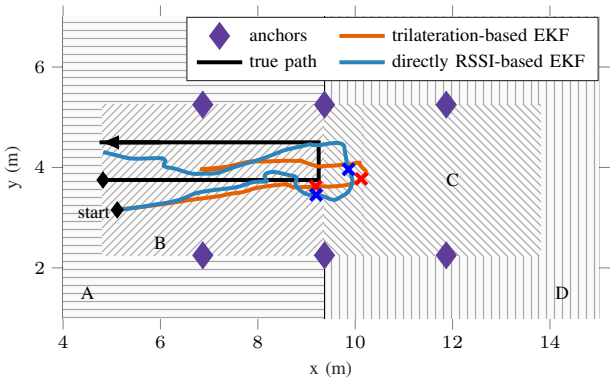

(a) Trajectories with marked position estimates of turning points.

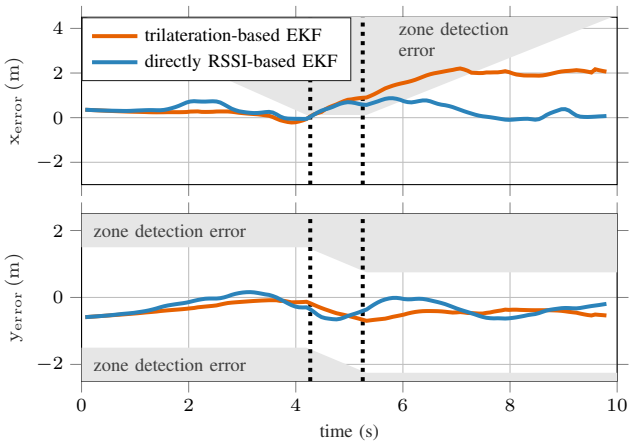

(b) Tracking error. Black dotted lines mark the turns.

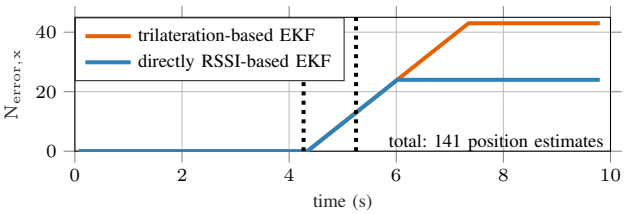

(c) Cumulated number of errors.
Black dotted lines mark the turns.

Fig. 6: EKF tracking results for a turn

the position-based method in this experiment. It shall further be noted here that trust in prediction and measurement is weighted by the Q- and R-matrices of the Kalman filter [11], which are commonly determined empirically. Especially the reliability of measurements has to be determined according to the setup: For instance, a higher anchor density improves reliability of RSSI measurements.

C. Using EKF with IMU

For orientation-dependent decision making in access control scenarios, the EKF approaches presented here are sufficient in most cases, especially the directly RSSI-based approach. For very challenging scenarios like unexpected movements at zone

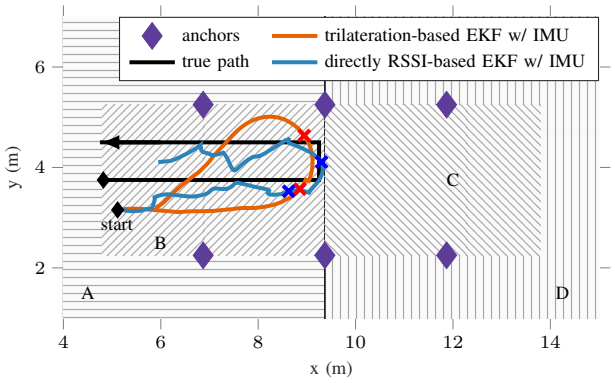

(a) Trajectories with marked position estimates of turning points.

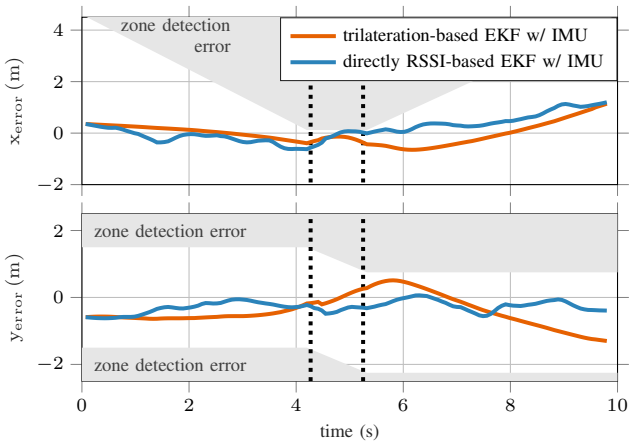

(b) Tracking error. Black dotted lines mark the turns.

Fig. 7: IMU-supported EKF tracking results for a turn

borders, additional information from the IMU can support the tracking, as shown in the following.

Using a smartphone as a mobile device comes with the advantage of an available inertial measurement unit (IMU). Adding the user's movement speed $\tilde{\mathbf{v}}$ and the IMU compass angle to the observation space (5),(6) and the measurement function of the filter (7),(8) fuses the sensor data with the position and RSSI. For a measurement of $\tilde{\mathbf{v}}$, pedestrian dead reckoning with step detection [13] was used. After measurement, the IMU data was transferred to the computer together with the RSSI measurements.

Comparing the IMU-supported tracking results for the turn trajectory with the purely RSSI-based filter performance, we observe a significant improvement: The change of the agent's orientation was detected earlier and thus no zone detection errors occurred in this case. Our observations thus confirmed the performance gain mentioned in the literature. As both RSSI as well as IMU data have to be present at the same unit for real-time tracking, a constant transfer of the agent's sensor data to the infrastructure is required. However, relying on the information broadcasted by the agent for security-related applications is risky as transmitted data may be manipulated.

IV. Additional Considerations

A. Calibration

In our experiments, using a calibration dataset obtained over a walk which mismatches the tracked movement induced more zone detection errors. In real-world applications, it is easily distinguishable from which side a user enters the gate. Thus we recommend an adaptive calibration scheme, which selects an appropriate set of system parameters from a stored pool of calibration data based on the starting point of the user. The calibration dataset could even be changed in online operation based on the user's movement: After a turn, calibration data could be switched to a parameter set obtained from a walk in the opposite direction.

B. Filter Initialization

The assumed initial state $\mathbf{x}_0$ of the filters has a crucial impact on the tracking performance. For a realistic evaluation of results, we need to assume some uncertainty of the initial state: The starting point for the filter was chosen randomly within a radius of $1\,\mathrm{m}$ around the true position. The initial movement speed was a random value between 0 and $1.6\,\frac{\mathrm{m}}{\mathrm{s}}$, and the agent's orientation was randomly chosen in an interval of $\pm 20^\circ$ around the true orientation. A priori knowledge about the surroundings, e.g. the position of doors through which a user enters the scene, can be used to determine suitable strict bounds for the initial state in a separate step.

C. Computational Complexity

Real-time tracking requires a fast computation of the position estimate. Thus, it is worthwhile to discuss the computational complexity of the proposed trilateration-based and direct approach. As trilateration estimates the position explicitly, a non-linear optimization problem is solved numerically in every step of the filter (cf. (2)). In comparison, the directly RSSI-based approach estimates the position implicitly by applying the path loss model in (8). The Jacobian of the measurement function, which is required for the linearisation of the problem in the EKF, is pre-calculated analytically and kept in memory. Consequently, the computationally expensive part reduces to a matrix inversion in the Kalman gain computation [11]. This results in a significantly reduced computational complexity for the directly RSSI-based approach.

V. Conclusion

In this paper, we have shown that BLE is a suitable technology for access control applications by demonstrating a low-complexity BLE-based user tracking system, including a suitable anchor constellation, diversity measures and recommendations for calibration. A system evaluation for various access control scenarios is possible with our proposed zone concept. In applications which require an accurate "inside/outside"-decision such as intruder detection, trilateration with a temporal moving-median filter already yields reliable decisions. If the user's intention needs to be predicted, e.g. in order to open automatic doors for authorized users, more advanced temporal filtering is required. Our directly RSSI-based EKF outperformed the computationally more expensive trilateration-based approach in the scenarios under investigation. We further demonstrated how additional sensor information from the agent's IMU can improve the tracking performance in security-wise uncritical applications.

Acknowledgment

We would like to thank C. Sulser for his support with measurements, and S. Pfister for developing the iOS application.

References

[1] Q. H. Nguyen, P. Johnson, T. T. Nguyen, and M. Randles, "Optimized indoor positioning for static mode smart devices using BLE," in *2017 IEEE 28th Annual International Symposium on Personal, Indoor, and Mobile Radio Communications (PIMRC)*, Oct 2017, pp. 1–6.

[2] J. Pelant, Z. Tlamsa, V. Benes, L. Polak, O. Kaller, L. Bolecek, J. Kufa, J. Sebesta, and T. Kratochvil, "BLE device indoor localization based on RSS fingerprinting mapped by propagation modes," in *2017 27th International Conference Radioelektronika (RADIOELEKTRONIKA)*, April 2017, pp. 1–5.

[3] W. Zhang, R. Sengupta, J. Fodero, and X. Li, "DeepPositioning: Intelligent Fusion of Pervasive Magnetic Field and WiFi Fingerprinting for Smartphone Indoor Localization via Deep Learning," in *2017 16th IEEE International Conference on Machine Learning and Applications (ICMLA)*, Dec 2017, pp. 7–13.

[4] D. Liang, Z. Zhang, A. Piao, and S. Zhang, "Indoor localization algorithm based on iterative grid clustering and AP scoring," in *2015 IEEE 26th Annual International Symposium on Personal, Indoor, and Mobile Radio Communications (PIMRC)*, Aug 2015, pp. 1997–2001.

[5] S. Yiu, M. Dashti, H. Claussen, and F. Perez-Cruz, "Wireless RSSI fingerprinting localization," *Signal Processing*, vol. 131, pp. 235 – 244, 2017. [Online]. Available: http://www.sciencedirect.com/science/article/pii/S0165168416301566

[6] O. Renaudin, T. Zemen, and T. Burgess, "Ray-Tracing Based Fingerprinting for Indoor Localization," in *2018 IEEE 19th International Workshop on Signal Processing Advances in Wireless Communications (SPAWC)*, June 2018, pp. 1–5.

[7] H. Bae, J. Oh, K. Lee, and J. H. Oh, "Low-cost indoor positioning system using BLE (Bluetooth low energy) based sensor fusion with constrained extended Kalman Filter," in *2016 IEEE International Conference on Robotics and Biomimetics (ROBIO)*, Dec 2016, pp. 939–945.

[8] S. P. Subramanian, J. Sommer, F. P. Zeh, S. Schmitt, and W. Rosenstiel, "PBIL PDR for scalable Bluetooth Indoor Localization," in *2009 Third International Conference on Next Generation Mobile Applications, Services and Technologies*, Sept 2009, pp. 170–175.

[9] H. Schulten, M. Kuhn, R. Heyn, G. Dumphart, F. Trösch, and A. Wittneben, "On the Crucial Impact of Antennas and Diversity on BLE RSSI-based Indoor Localization," in *Vehicular Technology Conference. IEEE 89th Vehicular Technology Conference. VTC Spring 2019*, April 2019.

[10] Y. Qi and H. Kobayashi, "On relation among time delay and signal strength based geolocation methods," in *Global Telecommunications Conference, 2003. GLOBECOM '03. IEEE*, vol. 7, Dec 2003, pp. 4079–4083 vol.7.

[11] I. Guvenc, C. Abdallah, R. Jordan, and O. Dedeoglu, "Enhancements to RSS Based Indoor Tracking Systems Using Kalman Filters," in *International Signal Processing Conference (ISPC) and Global Signal Processing Expo (GSPx)*, 2003.

[12] J. M. Castro-Arvizu, J. Vila-Valls, A. Moragrega, P. Closas, and J. A. Fernandez-Rubio, "Received signal strength-based indoor localization using a robust interacting multiple model–extended Kalman filter algorithm," *International Journal of Distributed Sensor Networks*, vol. 13, no. 8, 2017.

[13] N.-H. Ho, P. H. Truong, and G.-M. Jeong, "Step-Detection and Adaptive Step-Length Estimation for Pedestrian Dead-Reckoning at Various Walking Speeds Using a Smartphone," *Sensors*, vol. 9, 2016.